Supplemental Methods

Antibodies

EGFR (06-847) antibody (raised against an epitope in the C-terminal domain of EGFR) recognizes both EGFRwt and EGFRvIII and was purchased from Upstate/Millipore. β-actin (A206) antibody from sigma, β-actin (sc-47778), IKKγ or NEMO (sc-8330),TAK1 (sc-7162, sc-7967) RIP1 (sc-7881), tubulin (sc 8035) and FADD (sc 5558) were purchased from Santa Cruz Biotechnology . Phospho-EGFR antibodies (Tyr-1068, #2236), Caspase-8 (#9746) K63-linkage specific Polyubiquitin (#5621), IKK-γ/NEMO (#2695), cIAP1 (7065) antibodies were obtained from Cell Signaling Technology. RIP1 antibody from BD Biosciences (#610459), TRADD (ab74320), c-IAP2 (ab23423) from Abcam and TRAF-2 from Lifespan Biosciences (LS – B1427/10578).

Western blot and Immunoprecipitation

Protein lysates were prepared for Western blot using a lysis buffer containing, 1% NP-40, 150mM NaCl, 0.25 deoxycholate, 1mM EGTA, 1mM NaF, 50mM Tris-HCl, 1mM PMSF, 2mM orthovanadate, and a protease inhibitor cocktail. The same buffer was used for immunoprecipitation unless described otherwise. Immunoprecipitation was conducted according to standard protocols.

For analysis of RIP1 ubiquitination we followed a protocol described previously (Biton and Ashkenazi, 2011) and as described in supplemental methods. Briefly, cell lysates were made with RIPA lysis buffer containing 2mM N-Ethylmaleimide. After quantification, 1% SDS and 10mM NEM were added to the lysate which was boiled for 5 minutes at 95^0 C, diluted to a final concentration of 0.1% SDS with lysis buffer. Immunoprecipitation was conducted with RIP1 antibody followed by Western blot with K63-linkage specific Polyubiquitin antibody from Cell Signaling Technology.

RNA Isolation

Cells were incubated with or without Tetracycline (1ug/ml) for 24h. RNA extraction from cells or glioblastoma tissues was performed using the RNeasy kit from Qiagen. Only RNA samples with an A_{260}/A_{280} ratio $\geq$ 1.8 and with no visible degradation by agarose gel electrophoresis were used for RNA extraction and cDNA synthesis for Real Time PCR experiments.

cDNA Synthesis and Real Time PCR

cDNA was prepared from total RNA, using a combination of oligo-dT, random primers, dNTPs, and Superscript II (Invitrogen) and Superase.in (RNA inhibitor from Ambion). PCR primers for each gene were obtained from PrimerBank or were designed using Primer3 software, with a melting temperature at 58-60°C and a resulting product of approximately 100 bp. Each PCR was carried out in triplicate in a 20µl volume using SYBR Green Master Mix (Applied Biosystems, CA) for 15 minutes at 95°C for initial denaturing, followed by 40 cycles of 95°C for 15 s and 60°C for 60 s in the ABI prism 7700 sequence Detection system. cDNA prepared from Universal RNA (Stratagene, La Jolla, CA, USA) was used to construct a standard curve for each gene. Two independent experiments were done. Values for each gene were normalized to expression levels of 18S RNA. Primer sequences are below.

EGFR vIII-F
5' GGG CTC TGG AGG AAA AGA AAG GT 3'

EGFR vIII-R
5' CTT CTT ACA CTT GCG GAC GC 3'

Electrophoretic mobility shift assay

Briefly, 10 µg of nuclear extract from the cell-line was incubated with 0.5 f mol double-stranded 32P-labeled NF-κB oligonucleotide in the presence of 1µg of poly (dI-dC) in EMSA binding buffer for 30 min at 37^0C. The resulting DNA-protein complex was resolved in 6.6% non-denaturing polyacrylamide gel using EMSA running buffer at 150 volts for 3 h. The gels were dried in a gel drier and exposed to X-ray film and developed. The sequence of NF-κB

oligonucleotide used is 5'-TTG TTA CAA GGG ACT TTC CGC TGG GGA CTT TCC AGG GAG GCG TGG-3’

Limiting dilution of Glioma stem cell Cultures:

Glioma stem cell line was developed from the surgery samples (Singh SK, 2004) with modifications in stem cell medium (DMEM/F-12, 1:50 of B-27 supplement, 20 ng/ml hEGF, 20 ng/ml hFGF-b). Neurospheres were then dissociated into single cells by using Accutase (GIBCO). The cells were plated in 96 well plates by using limiting dilution (0.3 cells / 100µl) so that each neurosphere will arise from a single cell. Each well is considered as a single clone. Each clone has a capacity to proliferate, self-renew and forms secondary neurospheres. Each well was harvested separately in 6 well plates. Whole cell lysates were made from each individual clone separately and assessed for EGFR expression by Western Blot.

Cell proliferation Assays

Cells were plated at 20,000 per well in a 12-well tissue culture plate in the presence and absence of tetracycline (1µg/µl). The cells were trypsinized, analyzed by trypan blue exclusion for dead cells and counted using an automated cell counter after 72 h of plating.

MTT Conversion assay

An MTT conversion assay was done using a Roche Applied Bioscience kit according to the manufacturer’s protocol

Reference:

1. Singh SK et al (2004) Nature 432: 396-401.

Supplemental Figure Legends

Figure 1

A. U26 cells are derived from U87MG cells and express EGFRvIII conditionally in response to tetracycline. Expression of EGFRvIII in U26 cells results in increased phosphorylation of the p65 subunit of NF-κB. B. Activity of a transfected NF-κB luciferase reporter is high in GBM9-NS cells. Both Erlotinib and Necrostatin-1 inhibit NF-κB activity in these cells ($p<0.0001$, 1way ANOVA). C. U1 cells express EGFRvIII in response to tetracycline. EGFRvIII becomes constitutively autophosphorylated upon expression. We examined the effect of various concentrations of Erltonib on the kinase activity of EGFRvIII by conducing Western blots for phospho-EGFR (Tyr-1068). D. A dose response curve of the effect of Erlotinib on phosphorylation of EGFR. The phospho-EGFR signal on Western blot was quantitated by densitometry. E. Tyrphostin AG 1478 is another specific inhibitor of EGFR kinase and was used in a similar experiment at a concentration of 100nM, resulting in complete inhibition of EGFRvIII kinase activity. F. A reporter assay showing that the transcriptional activity of NF-κB is increased in tetracycline treated U26 cells. However, the tetracycline induced increase is abolished by exposure to EGF ($P <0.0001$, 1way ANOVA). G. NF-κB activity is increased in LN229 cells expressing EGFRvIII constitutively compared to LN229 cells transfected with empty vector. Addition of EGF results in a loss of EGFRvIII mediated NF-κB activity (1way ANOVA, $p=0.002$).

Figure 2

A. Electrophoretic mobility shift assay in U1 cells. Exposure of cells to tetracycline (24h) results in EGFRvIII expression and increased NF-κB DNA binding activity. Exposure of cells to EGF (50ng/ml) for 2h or 6h abolishes the EGFRvIII induced NF-κB DNA binding activity. B. U251vIII cells express conditionally express EGFRvIII in response to tetracycline. U251vIII also express

endogenous EGFRwt. In this experiment we selectively silenced EGFRwt in U251vIII cells by using shRNA directed against exon 3 in EGFRwt (exon 3 is missing in EGFRvIII). We used control (scrambled) shRNA as a control. Western blot showing effective silencing of EGFRwt in U251vIIIshwt cells while the U251vIIIshC cells show the endogenous EGFRwt expressed in these cells. C. Next, we conducted a reporter assay examining the transcriptional activity of NF-κB in these cells in response to EGF. Exposure of U251vIIIshC cells to EGF leads to a sharp drop in reporter activity ($p \leq 0.0001$, Tukey's Multiple Comparison Test) (EGF 50ng/ml, 6h). However, EGF does not decrease the NF-κB reporter activity in U251vIIIshwt cells, indicating that EGF acts via the EGFRwt in these cells. Renilla luciferase was used as an internal control.

Figure 3

Single cell suspensions were generated from neurosphere cultures of GBM9-NS and GBM748-NS. Both these tumors express both EGFRwt and EGFRvIII. A. Four clones derived from single cells from GBM9-NS show that in each clone there is co-expression of both EGFRwt and EGFRvIII. Lysates from U251vIII cells with or without tetracycline were run to show the relative positions of EGFRwt (no tetracycline) and EGFRvIII (tetracycline) conditions. B. Four clones derived from single cells from GBM748-NS show that in each clone there is co-expression of both EGFRwt and EGFRvIII. The U87MG lane shows the position of EGFRwt while the U251vIII+tet lane shows the position of EGFRvIII in the gel.

Figure 4

RIP1 is essential for EGFRvIII mediated activation of NF-κB transcriptional activity in U251-vIII cells. A. siRNA mediated knockdown of RIP1 blocks the ability of EGFRvIII to activate NF-κB. Addition of tetracycline results in expression of EGFRvIII in both RIP1 silenced and control (scrambled) siRNA control but NF-κB is activated only in control siRNA cells ($p=0.001$). B. Silencing of RIP1 is shown by Western blot. C. EGFRvIII mediated transcriptional activity of

NF-κB is blocked by Necrostatin-1 in U251vIII cells (p=0.0001). D. We examined the effect of various concentrations of Necrostatin-1 on the kinase activity of RIP1 by conducing Western blots for phosphorylation of the p65 subunit of NF-κB in U1 cells. E. A dose response curve of the effect of Necrostatin-1 on phosphorylation of p65. The p65 signal on Western blot was quantitated by densitometry. F. This result was validated with siRNA knockdown of RIP1. Silencing of RIP1 decreases EGFRvIII mediated phosphorylation of the p65 subunit of NF-κB in U1 cells.

Figure 5

A. A cell counting experiment demonstrating that RIP shRNA clone L11 cells proliferate slowly in cell culture compared to Control shRNA expressing cells (1way ANOVA, p=0.0046). Cell death was excluded by trypan blue exclusion prior to automated cell counting. B. The same experiment was conducted in clone S1 (1way ANOVA, p=0.0011). C. An MTT conversion assay was conducted comparing U1 cells with stably silenced RIP1 (L11) to U1 cells with control shRNA. MTT conversion is higher in control cells compared RIP1 silenced cells suggesting increased proliferation in control cells (two tailed t test, p=0.002). Cell death was excluded by trypan blue exclusion in parallel experiments. D. U251vIII cells were exposed to tetracycline, with or without EGF (50ng/ml) as indicated followed by denaturation and IP with RIP1 and Western blot with K63 ubiquitin antibodies or RIP1 antibodies. The level of K63-linked ubiquitination of RIP1 is high in these cells and does not increase with tetracycline. However, a loss of K63-linked ubiquitination of RIP1 is seen in these cells after prolonged EGF exposure (24h). E. U1 cells were engineered to stably and constitutively express high levels of EGFR wild type (U1wt cells). Thus, U1wt cells express high levels of EGFRwt constitutively and EGFRvIII in response to tetracycline (lanes 1-4). Lanes 5 and 6 show EGFR levels in actual GBM tumors (GBM6 and GBM9). Lysates were made directly from resected tumor tissue. Two

exposures are shown to demonstrate the separation of EGFRwt from EGFRvIII and also to show the endogenous EGFRwt in U1 cells.

Figure 6

A. U1wt cells were exposed to EGF for 72 hours. There is no cell death in the absence of EGF. When EGF is added for 72h, there is substantial cell death (tet+EGF) shown by the decrease in the number of viable cells ($p<0.0001$), with most of the cell death being necrotic as shown by the PI positive cells ($p<0.0001$). Addition of RIP1 kinase inhibitor Necrostatin-1 inhibits EGF induced necrotic cell death (tet+EGF+necrostatin). As a control for Necrostatin-1 cells were treated with DMSO in tet+EGF cells. Data were analyzed by 1way ANOVA followed by Newman-Keuls Multiple Comparison test. B. Effective silencing of RIP1 in U1 cells was confirmed with a Western blot for the experiment shown in Figure 6C-E. C. Stable overexpression of EGFRwt in U251vIII cells. U251vIII cells were stably transfected with control vector or EGFRwt. U251vIIIwt cells overexpress EGFRwt compared to U251vIIIC cells that express endogenous EGFRwt. D. When U251vIIIwt cells are exposed to EGF, they undergo cell death that is largely necrotic (PI positive cells). If the RIP1 inhibitor, Necrostatin-1 is used (300nM), EGF no longer induces cell death. The data were analyzed by one way analysis of variance (ANOVA) followed by Newman-Keuls Multiple Comparison Test. Cell viability is decreased in Tet +EGF condition ($p\leq0.0001$) in comparison to no Tet/Tet and Tet+EGF+Necrostatin conditions. There is a significant increase in PI positive cells after EGF treatment in Tet+EGF group, when compared to no Tet/ Tet and Tet+EGF+Necrostatin conditions ($p\leq0.0001$). E. EGF abolishes EGFRvIII mediated NF-κB activation in U1wt cells. Expression of EGFRvIII by exposure of cells to tetracycline results in NF-κB activation as assessed by a NF-κB reporter assay. Addition of EGF to cells results in a loss of EGFRvIII-mediated NF-κB activation. This is consistent with the results found in U1 cells. F. EGF mediates increased association of FADD and RIP1 in U1wt cells for up to 24h.

Immunoprecipitation of FADD was followed by Western blot with RIP1 antibodies. G. Caspase-8 is complexed with RIP1 in U1wt cells and this association does not change significantly with EGF over time.

Figure 7

A. FACS plot original data for the graph shown in Figure 6A and B.

B. Quantitative real time PCR was performed to detect EGFRvIII in RNA extracted from individual tumors. Increased EGFRvIII can be detected by qPCR in all tumor samples demonstrating expression of EGFRvIII by Western blot except for GBM4.

Supplemental Figure 1

Puliyappadamba et al.

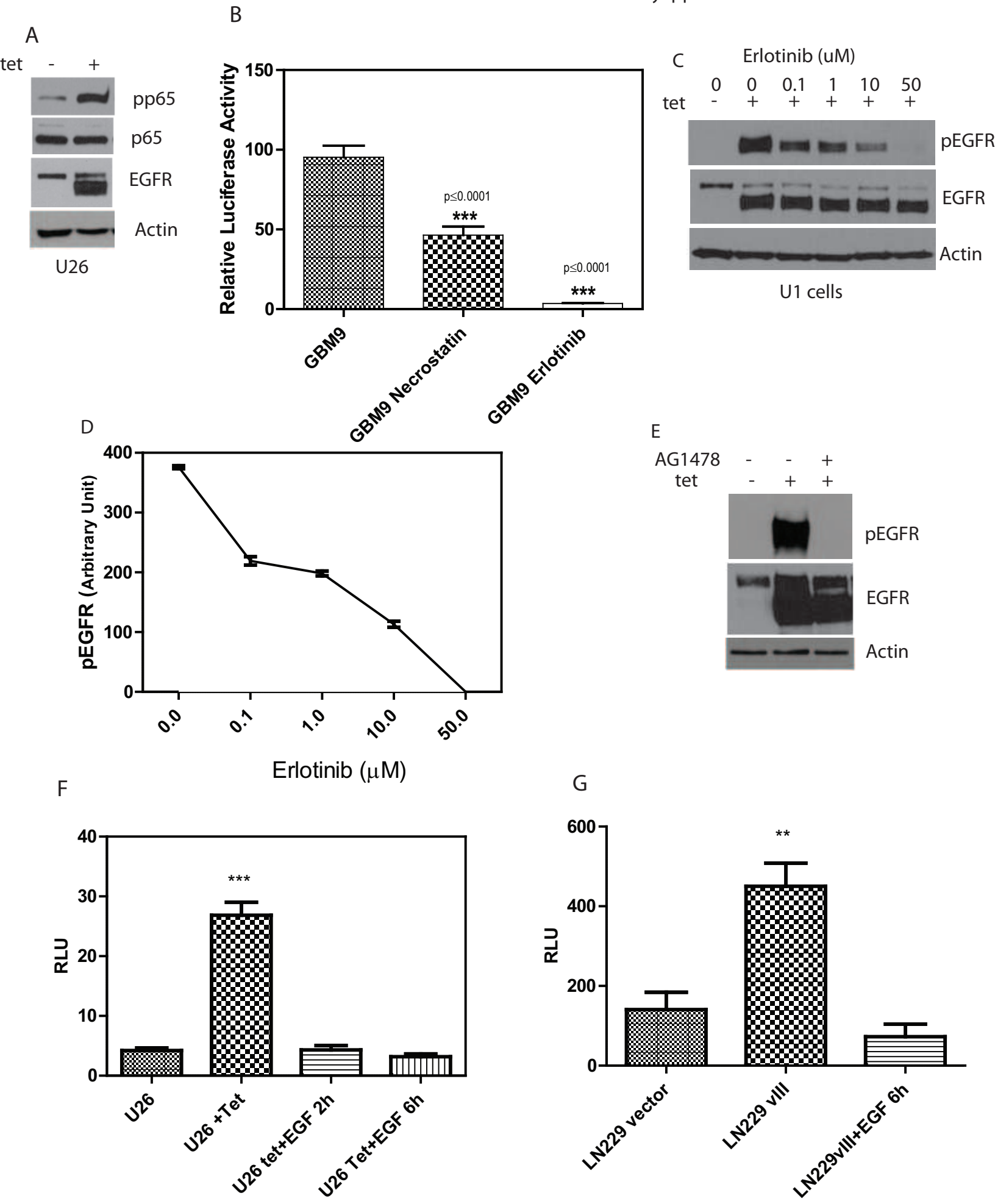

Supplemental Figure 2

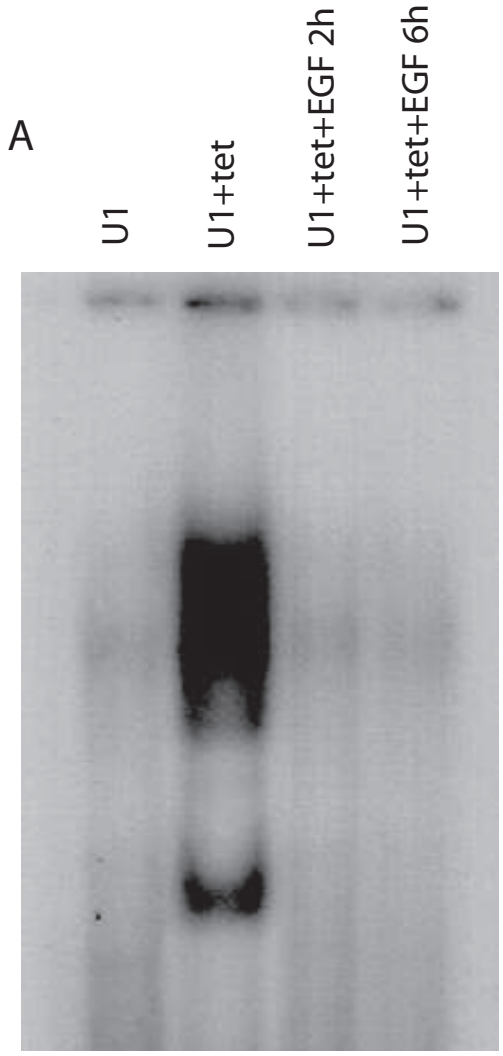

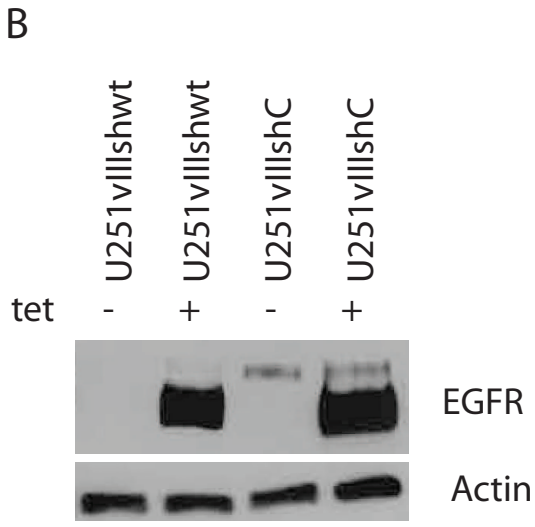

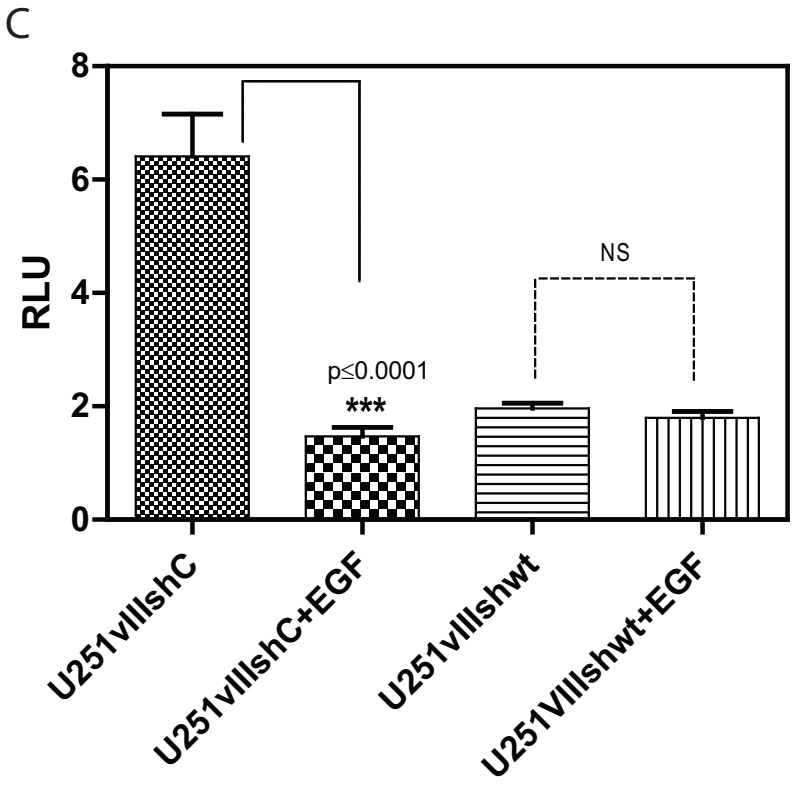

Supplemental Figure 3

Puliyappadamba et al

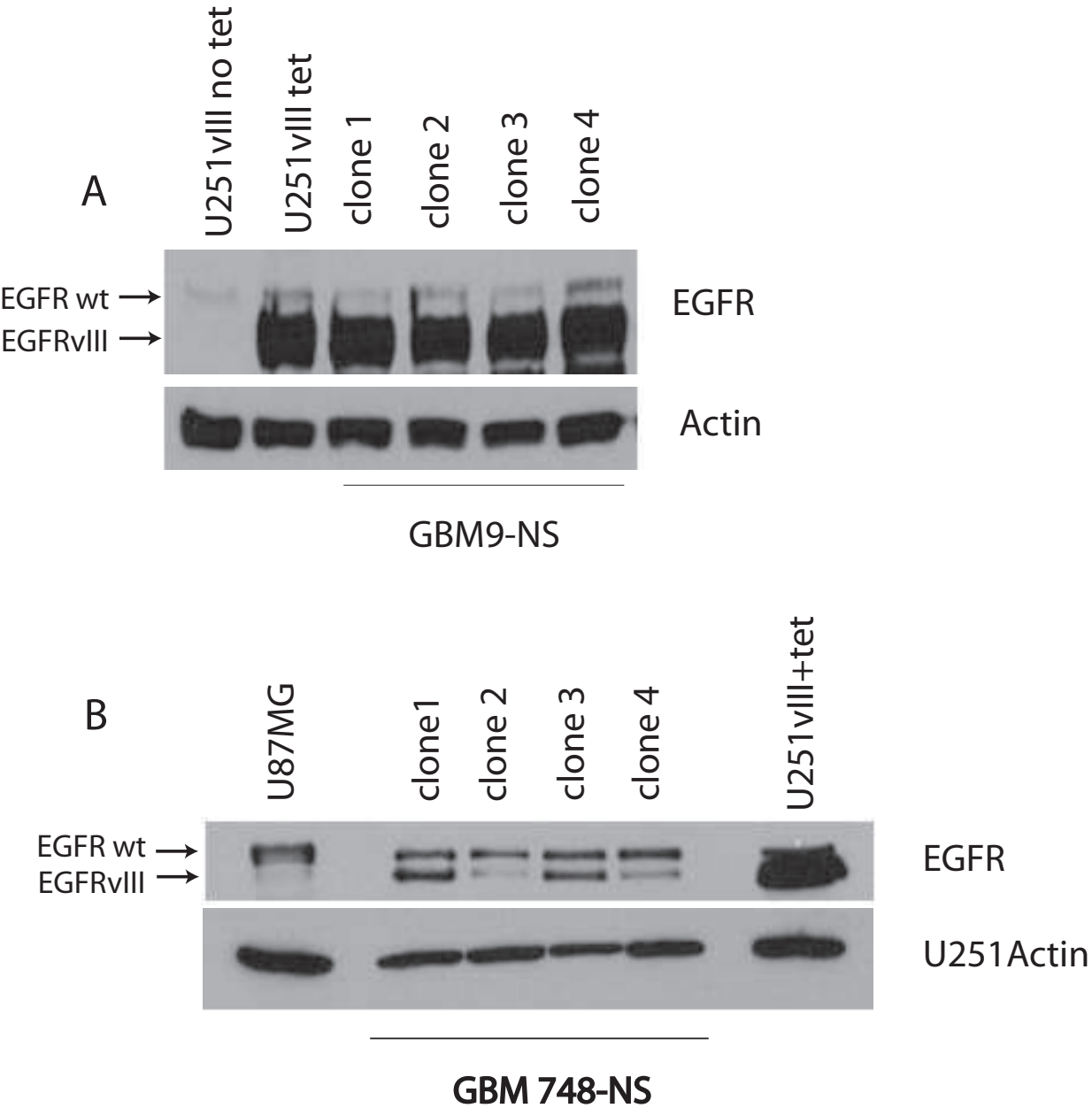

Supplemental Figure 4

Puliyappadamba et al.

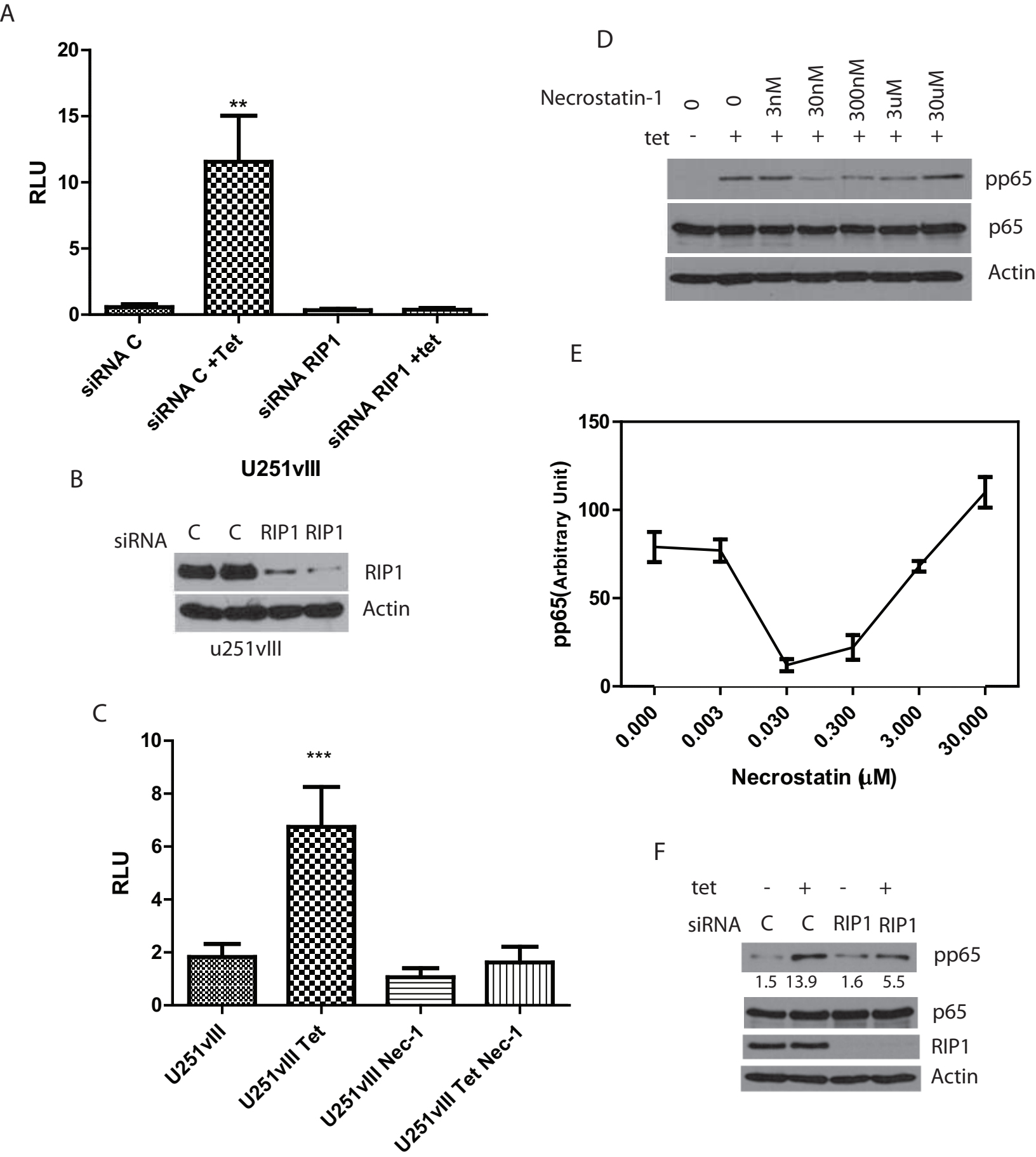

Supplemental Figure 5

Puliyappadamba et al.

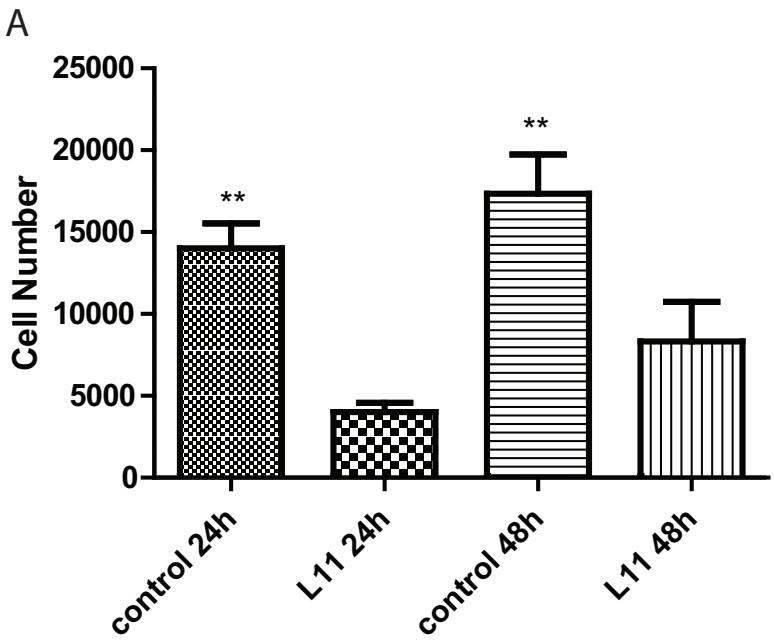

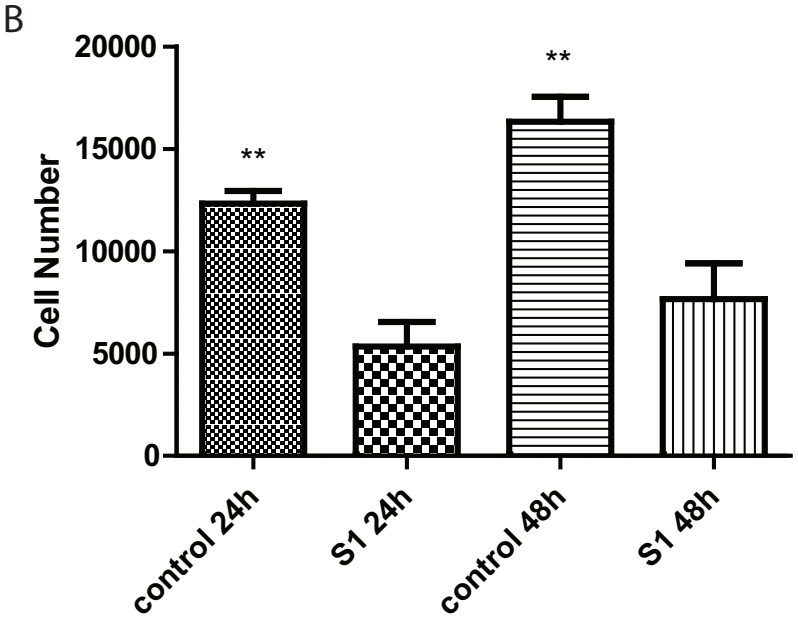

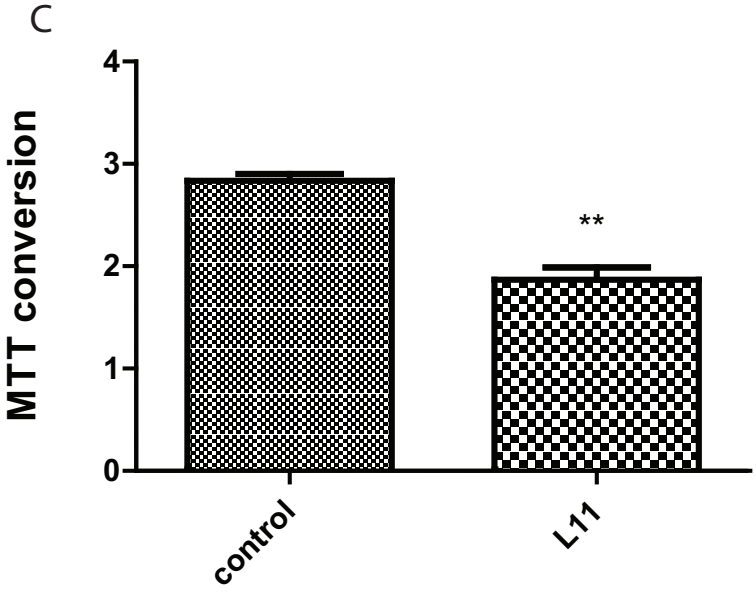

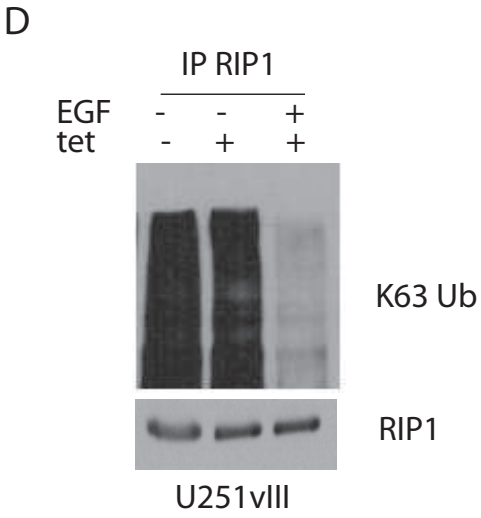

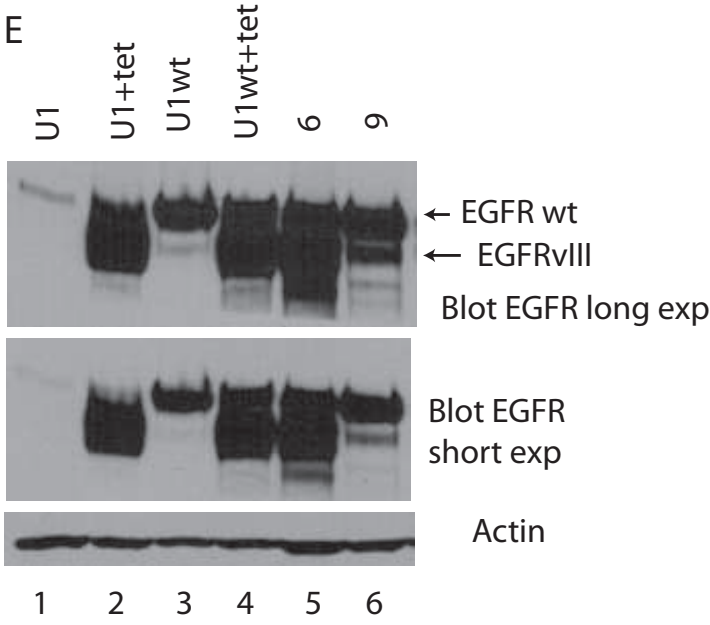

Puliyappadamba et al.

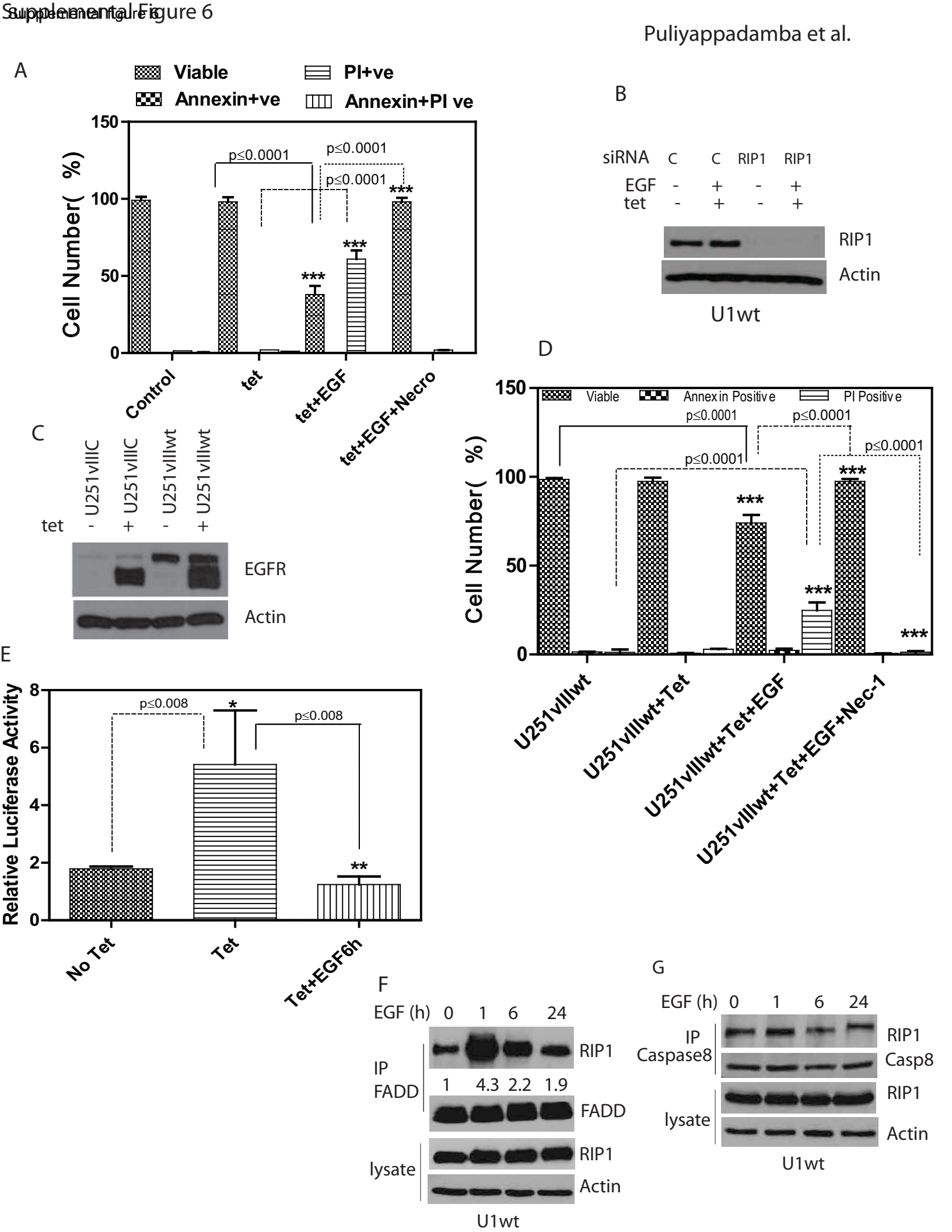

A

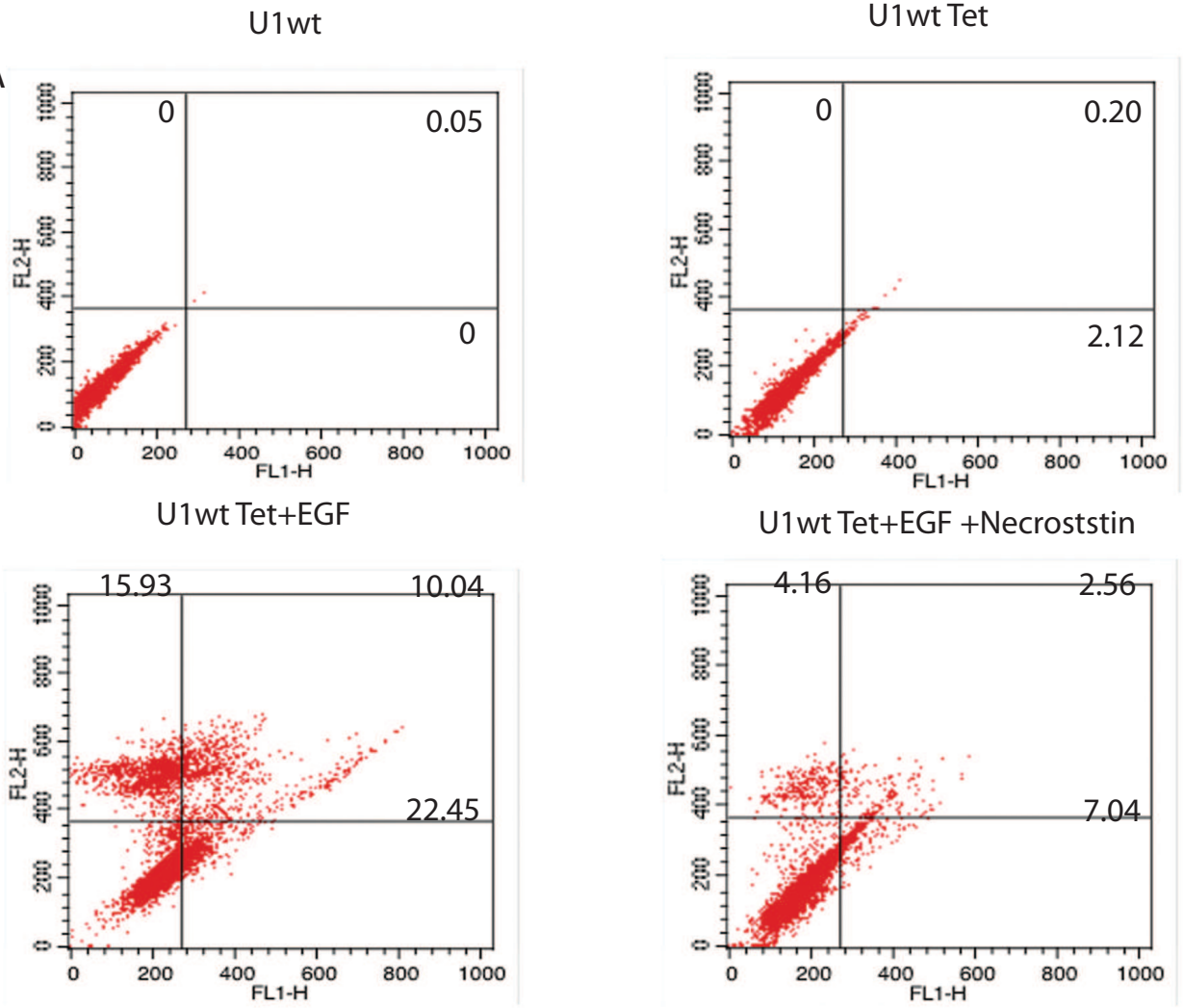

FL1-H Annexin, FL2-H Propidium Iodide

Lower Left -Unstained,
Lower Right -Annexin Positive
Upper Left -Propidium Iodide
Upper Right-Annexin +Propidium Iodide

B